JAAS
Journal of Analytical Atomic Spectrometry

Accepted Manuscript

This article can be cited before page numbers have been issued, to do this please use: E. Ender, M. A. Subirana, A. Raab, E. Krupp, D. Schaumlöffel and J. Feldmann, *J. Anal. At. Spectrom.*, 2019, DOI: 10.1039/C9JA00187E.

ROYAL SOCIETY OF CHEMISTRY

rsc.li/jaas

View Article Online
DOI: 10.1039/C9JA00187E

Why is NanoSIMS elemental imaging of arsenic in seaweed (*Laminaria digitata*) important for understanding of arsenic biochemistry in addition of speciation information?

E. Ender[1], M.A.Subirana[2], A. Raab[1], E.M. Krupp[1], D. Schaumlöffel[2], J. Feldmann[1]

[1]*TESLA, School of Natural and Computing Sciences, University of Aberdeen, Aberdeen AB24 3UE, Scotland, UK*

[2]*CNRS / Université de Pau et des Pays de l'Adour / E2S UPPA, Institut des Sciences Analytiques et de Physico-Chimie pour l'Environnement et les Matériaux, UMR 5254, 64000 Pau, France*

Abstract

Brown seaweed such as *Laminaria digitata* is known to accumulate arsenic to more than 100 mg/kg. How the algae can tolerate such high level of arsenic has traditionally been studied by arsenic speciation analysis using HPLC-ICPMS, but the knowledge of its molecular forms has not yet given any answers. Here we demonstrate for the first time that the combination of speciation analysis with high resolution imaging by NanoSIMS and TEM identifies not only the molecular structures of arsenic but also the location of arsenic in cells and cell substructures in a brown seaweed species.

The majority of 117 mg/kg arsenic in *L. digitata* fronds was in the form of inorganic arsenic (53%) and arsenosugars (32%) and only 1.5% of total arsenic as arsenolipids (mainly as AsHC and AsPL). The lateral resolution of 300 nm and the concentration of arsenic was high enough for the localization of arsenic in the cells of the seaweed using NanoSIMS. The majority of arsenic was found in the cell walls and cell membrane, while the inside of the cell was almost arsenic free, which is not expected if the majority of arsenic species are hydrophilic. The NanoSIMS images questions the integrity of the arsenic species during extraction for the speciation analysis and that inorganic arsenic is unlikely to occur freely in the seaweed. Whether inorganic arsenic and the arsenosugars are bound directly to the polymeric carbohydrates alginates or fucoidans in the seaweed is unclear and needs further investigations.

View Article Online
DOI: 10.1039/C9JA00187E

Introduction

The use of analytical atomic spectrometry and in particular ICPMS has been instrumental to identify the molecular forms of arsenic in biological samples over nearly three decades. The complex arsenic biochemistry of more than 100 naturally occurring organoarsenicals in addition to arsenite and arsenate made it necessary to use various HPLC methods coupled to ICPMS and ESI-MS detection in off-line or on-line mode to identify the full spectrum of arsenic species in biological samples even without standards.[i] However, neither the biosynthetic pathways nor the classification whether these metabolic transformations are detoxification pathways for inorganic arsenic or the formation of beneficial arsenic containing biomolecules have been elucidated; although credible suggestions have recently been made about the arsenosugars.[ii] What is missing is the localisation of the arsenic inside the cells in order to answer the above mentioned questions about the biochemistry of arsenic.

It is well known that seaweeds bioaccumulate large concentrations of arsenic from seawater with bioconcentration factor between 1,000 and 100,000.[iii] Seaweeds and in particular brown macroalgae can reach concentrations up to 200 mg As/kg.[iv] Most of the arsenic in seaweeds is present as organoarsenicals in the form of arsenosugars (As-sugars), dimethylarsinic acid (DMA) and also in the lipid soluble forms of arsenic containing hydrocarbons (AsHC), fatty acids (AsFA) and phospholipids (AsPL)[v,vi]. Only *Hijiki* spp [vii]and *Laminaria digitata* [viii,ix] seem to contain large amounts of inorganic arsenic.

Here we would like to illustrate the complementary information of using detailed arsenic speciation analysis and mapping of arsenic at sub-cellular level using the brown seaweeds *Laminaria digitata* as examples to gain more detailed insight into the bioaccumulative behaviour of arsenic especially when the arsenic species are known. Special attention will be given to the differences in the sample preparation procedures. While often the samples are freeze-dried before speciation analysis by HPLC-ICPMS is performed in order to report on concentration relative to dry mass, is it important to have fresh samples available for transmission electron microscope (TEM) and nanoscale secondary ion mass spectrometry (NanoSIMS) analysis which need to be prepared by cryofixation using high-pressure freezing followed by cryo-substitution and resin embedding. This is necessary in order to conserve the cellular ultrastructure and to fix the elements and not distribute them at a sub-cellular level.

View Article Online
DOI: 10.1039/C9JA00187E

Experimental Section

Chemicals and reagents

All chemicals and reagents were purchased from Sigma-Aldrich (Saint-Quentin Fallavier, France) unless stated otherwise. All solutions, dilutions and preparations were made with water (18.2 MΩ cm) obtained from a Milli-Q system (Millipore, Bedford, Ma, USA) unless stated otherwise. A 10 µL drop of an arsenic ICP Standard, 1000 µg/mL (PlasmaCAL, Villebon-sur-Yvette, France), was dried on a silica wafer and used as standard for mass calibration and mass resolution tuning for As in NanoSIMS.

Chemicals used for extraction were of lab-grade quality (Fisher, UK). Chemicals used for total As determination were of trace-element grade (VWR, UK). HPLC grade methanol (Rathburn, UK), ammonium carbonate (Sigma, UK) and formic acid (mass-spec quality, Fluka, UK) were used for the preparation of HPLC eluents. Nitric acid (70 % p.a. Fisher, UK) and hydrogen peroxide (32 % Fisher, UK) were used for extraction and digestion. For quantification of As-species sodium dimethylarsinic acid (DMA, Chemservice, USA) was dissolved in deionized water and diluted as necessary. Identification of anionic As-species was aided by species standards of DMA, MA (Chemservice, USA), arsenite and arsenate (BDH, UK). Seaweed CRM (ERM-CD-200) a brown algae *Fucus vesiculosus* was purchased from JRC-Institute for Reference Materials and Measurements (Geel, Belgium).

Samples

Sampling was conducted at a beach south of Aberdeen, on the east coast of Scotland (57.139856 N, -2.051430 W) in November 2018. Freshly washed ashore whole thalli of *Laminaria digitata* were harvested.

Sample preparation for NanoSIMS and TEM

Sample preparation was conducted at the Microscopy and Histology Core Facility at the University of Aberdeen. Two replicates of *L. digitata* were prepared. Algae discs of 4 mm diameter were prepared with a biopsy punch and transferred into gold-plated copper specimen carriers filled with hexadecane. High Pressure Freezing was then carried out using a Leica EM ICE (Leica Microsystems, Milton Keynes, UK). For freeze substitution samples were post-fixed with 2% osmium tetroxide (OsO_4) in acetone and transferred into an automatic freeze substitution system (AFS 2, Leica Mircosystems) following the programme outlined in Supplementary material. This was followed by resin embedding (Spurr's resin, TAAB, UK)

through a stepwise infiltration of the samples with a graded resin and acetone series (10, 30, 50, 70, and 90% resin in acetone). Finally, embedded in 100% resin the samples were polymerized at 60 °C for at least 24 hours. For TEM analysis, 90 nm sections were cut from the resin blocks using a diamond knife (Diatome Ltd, Switzerland) on an ultra-microtome (Leica UC6, Leica Microsystems) and placed onto copper grids (TAAB, UK). For NanoSIMS analysis, 300 nm sections were cut by the same method and placed on silicon wafers (Wafer Solution, Le Bourget du lac, France).

Sample preparation for totals arsenic analysis and speciation analysis

Laminaria digitata fronds were cleaned by scraping and washing off epiphytes and sediment, freeze dried and ground with mortar and pestle to a fine powder. Only the young fronts were analysed.

Extraction of lipophilic arsenic

Algae (1 g) were extracted with hexane (2 × 5 mL), followed by CH_2Cl_2/MeOH (2:1 v/v, 2 × 5 mL), and both extracts were evaporated to dryness. For speciation analysis only the MeOH soluble part of the CH_2Cl_2/MeOH extract was used.

Extraction of hydrophilic arsenic

The procedure of Petursdottir *et al*.[x] was used for the extraction. In brief 0.1 g algae were mixed with 10 mL of extraction solution (1 % (v/v) nitric acid and 2 % (v/v) hydrogen peroxide) and heated in a microwave (Mars5, CEM, UK) to 95ºC for 30 min. The solution was centrifuged and the supernatant used for determination of inorganic arsenic.

Digestion method to determine total arsenic

Total As was determined after standard microwave digestion with HNO_3/H_2O_2 using a Mars5 system (CEM, UK) in solid *L. digitata*. An ICPMS/MS (Agilent 8800, UK) was used in mass shift mode to determine As on m/z 91 as AsO^+ .

Determination of hydrophilic and lipophilic arsenic species

Hydrophilic arsenic species were determined by using anion exchange HPLC-ICPMS/MS. The parameters are given in the supplementary material. The lipophilic arsenic speciation was performed by coupling reverse-phase HPLC simultaneously to ICPMS/MS and ESI-qTOF-MS as described previously[xi]. The details are given in the supplementary material.

View Article Online
DOI: 10.1039/C9JA00187E

TEM analysis

Samples were viewed on the transmission electron microscopes JEM 1400 plus (JEOL, UK) at an accelerating voltage of 100 kV using an AMT UltraVUE camera. The TEM instrument was used to determine quality of sample preparation and for high resolution imaging of sub-cellular structures. Copper grids have been used for sample sections.

NanoSIMS analysis

A NanoSIMS 50L (Cameca, Gennevilliers, France) was used for high resolution secondary ion mass spectrometry analysis. A primary Cs^+ ion source served for the mapping of electronegative elements. Detectors were tuned for carbon ($^{12}C_2^-$), nitrogen ($^{12}C^{14}N^-$), phosphorus ($^{31}P^-$), sulphur ($^{32}S^-$) and arsenic ($^{75}As^-$). As the concentration of As in the sample was relatively low, an As standard was used for mass calibration and mass resolution tuning process. Cs^+ ions were implanted onto the sample surface in order to increase sensitivity. It should be noted that N cannot be directly measured using NanoSIMS, therefore carbon-nitrogen (CN^-) cluster ions are measured to detect N in the sample. Images were acquired with a raster size ranging of 35 µm, divided into 512 x 512 pixels with a dwell time of 10 ms per pixel. Individual sample sections were located using the NanoSIMS Charged Coupled Device (CCD) camera. The field of view of the CCD camera is about 500 × 600 µm and the optical resolution around 1 µm, which allows for an overview of the sample and a selection of regions of interest for NanoSIMS analysis.

Results and discussion

The arsenic concentration in the freeze-dried *L. digitata* was 117 +/- 30 mg As/kg (Table 1), which is in the normal range as reported previously.[viii] The accuracy and precision of the total arsenic was evaluated using a seaweed CRM and the recovery was quantitative.

Speciation analysis

The speciation of the hydrophilic fraction of arsenic gave the expected distribution of arsenic species, with 53% of the total arsenic in the form of inorganic arsenic (62 +/- 19 mg As/kg). Arsenosugars in the form of As-sugars (-glycerol, phosphate ester and sulfonate) contributed 32% (37 mg As/kg), while DMA was only a minor compound with less than 1 % of total As.

The arsenolipid fraction contributed also only 1.5% of total arsenic of which the majority 65% was in the form of arsenosugar containing phospholipids (AsPL) (structures see Figure 1). The identification and quantification was done using RP-HPLC-ICPMS/MS coupled simultaneously to ESI-MS. The assignment of the arsenic peaks was achieved by using the retention time as the first criteria, which should coexist with the corresponding protonated mass of the molecular mass (ESI-MS) as can be seen in Figure S1a and S1b (supplementary material). Further evidence for the identification were the accurate masses and MS/MS pattern as described by previously by Raab et al.[xii], where the arsenolipid profile of a brown seaweed *Saccharina latissima* was studied in detail.

Table 1: Total arsenic and hydrophilic arsenic species quantified; total arsenic (iAs), inorganic arsenic determined as arsenate (iAs), Sum of all arsenosugars (As-Sugar). Fractions are given as mass % of tAs. Errors are given as +/- SD for n=3.

	tAs	tAs_{hydro} (hydrophilic)	iAs	DMA	As-Sugar (sum)
	mg As/kg	mg As/kg	mg As/kg	mg As/kg	mg As/kg
*CRM CD-200**	55 ± 1.0	44 ± 0.67	0.090 ± 0.010	8.6 ± 0.3	32
L. digitata	117 ± 30	100 ± 22 *(85.5%)*	62 ± 19 *(53.0%)*	0.93 ± 0.11 *(0.8%)*	37 ± 3.9 *(31.6%)*

*certified reference value for tAs: 55 ± 4.0 mg/kg

Table 2: Total arsenic and arsenolipids quantified; arsenic containing hydrocarbons (AsHC), arsenosugar containing phospholipids (AsPL).

	tAs_{lipid} (lipophilic)	AsHC (sum)	AsPL (sum)
^{as} mg As/kg	1.7 ± 0.22	0.14 *(8.2%)*[a]	1.1 *(65%)*[a]
Mass % of total As	1.5%	0.12%	0.94%

[a] (% of As_{lipid})

View Article Online
DOI: 10.1039/C9JA00187E

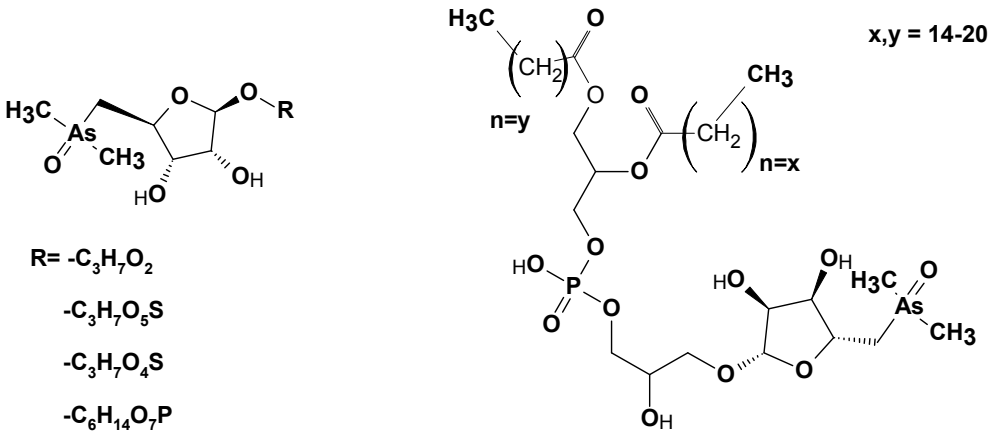

Figure 1: generic structures of major organoarsenic compounds in *L. digitata*: arsenosugar (As-sugar; left), arsenosugar containing phospholipid (AsPL; right)

Table 3: identified As-lipids and their concentration using the ICPMS signal and compound-independent quantification (n=3).

detected arsenolipid*	detected accurate mass**	µg As / kg algae dry mass
(AsFA422)	$C_{22}H_{36}AsO_3$ (m/z 423)	4.2 ± 0.12
(AsHC360)	$C_{19}H_{42}AsO$ (m/z 361)	71 ± 6.7
(AsHC374)	$C_{20}H_{44}AsO$ (m/z 375)	23 ± 5.3
(AsHC388 + AsHC402)	$C_{21}H_{46}AsO$ (m/z 389) + $C_{22}H_{48}AsO$ (m/z 403)	18 ± 2.4
(AsPL930)	$C_{43}H_{84}AsO_{14}P$ (m/z 931)	109 ± 14
(AsPL944)	$C_{44}H_{86}AsO_{14}P$ (m/z 945)	69 ± 11
(AsPL958)	$C_{45}H_{88}AsO_{14}P$ (m/z 959)	636 ± 93
(AsPL972)	$C_{46}H_{90}AsO_{14}P$ (m/z 973)	30 ± 4.4
(AsPL986)	$C_{47}H_{92}AsO_{14}P$ (m/z 987)	97 ± 13
(AsPL1000)	$C_{48}H_{94}AsO_{14}P$ (m/z 1001)	14 ± 1.7
(AsPL1014)	$C_{49}H_{96}AsO_{14}P$ (m/z 1015)	119 ± 18

*number in parentheses gives the non-protonated molecular mass
**For more information of the As-lipid structures see Raab et al. 2013[vi]

TEM analysis

The cells of *L. digitata* were imaged with transmission electron microscopy (TEM) and ultra-structures such as the nucleus, Golgi apparatus, chloroplast, and vacuoles were clearly detectable (Figure 2). Most prominent, very thick cell walls were observed which are characteristic for brown algae. These cell walls are adjacent to the cell membrane and consist of an amorphous matrix of alginates and fucoidans with a fibrillary skeleton of cellulose in the inner cell wall.[xiii,xiv] The amorphous outer cell wall can be also regarded as intercellular material.[xv] Alginate is an unbranched anionic polysaccharide comprised of two uronic acids: mannuronic acid and guluronic acid. Fucoidans are sulphated fucose-containing

polysaccharides containing -SO_3H groups. Cellulose accounts for only 1-8% of the algal dry mass, while fucoidans and alginates represent up to 45%.[xvi] Moreover, fucoidans play a role in algal cell wall organization and could be involved in the cross linkage of alginate and cellulose. Alginate gives flexibility to algae, serves as a structural support crosslinked by cationic metal ions and bound to proteins, and prevents desiccation. In addition, alginate is involved in the exchange of ions with seawater; it absorbs and retains polyvalent cations at concentrations significantly higher than those in the surrounding water.[xvii]

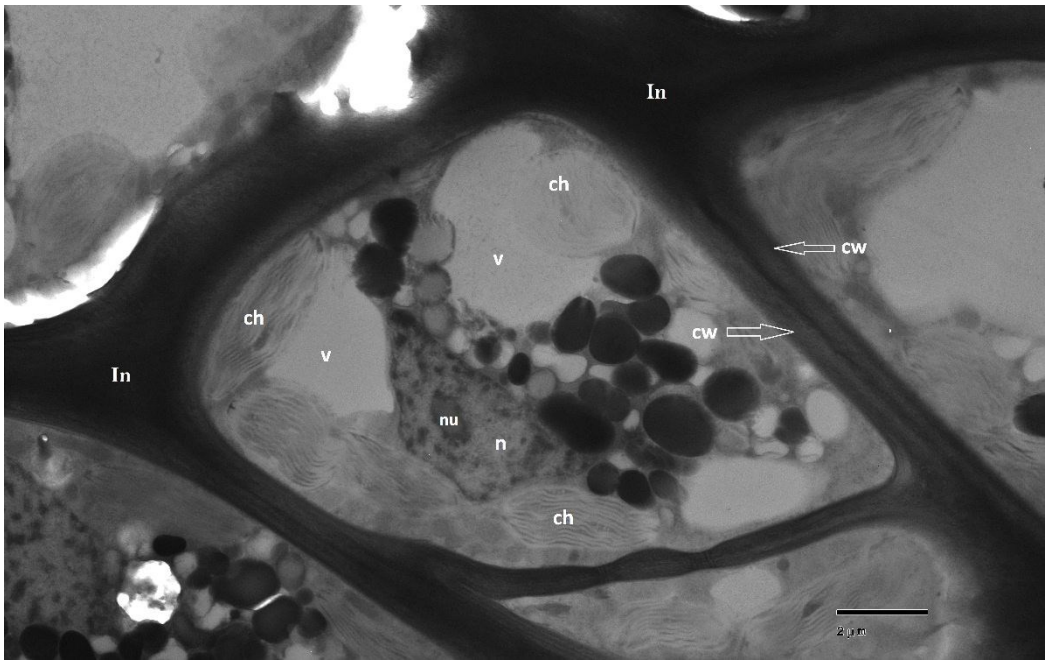

Figure 2. *TEM image obtained from 90 nm section of resin embedded L. digitata cell. Image is of the whole cell including, inner cell wall (cw) and amorphous outer cell wall (intercellular material (In)), cell membrane, vacuoles (v), nucleus (n), nucleolus (nu), chloroplasts (ch)). Bar length is 2 μm.*

Optimization of the NanoSIMS analysis method

The NanoSIMS analysis method has been optimized with regard to maximal spatial/lateral resolution for sub-cellular imaging and high sensitivity for detection of arsenic at trace level. For high lateral resolution the Cs^+ primary ion beam was trimmed using a diaphragm (D1-4) with a circled aperture of 150 µm and finally focused with the primary focusing lens (EOP) to its final spot size of about 50 nm at the sample surface. This lateral resolution was confirmed in our previous work by applying the knife-edge method on a standard sample[xviii] and is in agreement with the instrument specifications. In this work, the actual lateral resolution in the

View Article Online
DOI: 10.1039/C9JA00187E

image of the seaweed sample was determined by line scans at a sharp edge in the CN^- and S^- images (Figures 3ib and 4iia) using the 16-84% criterion (knife-edge method). Depending on the location in the image the actual resolution was about 300 to 400 nm. Note, that in biological samples not only the NanoSIMS primary beam size, but also the structure of the sample as well as the quality of sample preparation which influences the element distribution in the sample structure contributes to the measured lateral resolution. Therefore in biological samples usually a lower resolution is measured than in standards for the knife-edge method. The selected pixel numbers (512 x 512) for a 35 µm x 35 µm image results in a theoretical pixel size of 68 nm which is slightly higher than the smallest possible probe size of 50 nm but largely sufficient in view of the measured actual lateral resolution for mapping subcellular structures in seaweed cells.

An advantage of the NanoSIMS is that it combines high lateral resolution with high sensitivity. In order to accumulate a sufficient number of counts for the detection of trace amounts of arsenic a compromise had to be found between the dwell time of the primary beam per pixel, the number of accumulated image scans (planes), and a reasonable analysis time in which the thin sample section of 300 nm was not completely consumed. Note that NanoSIMS is a destructive technique where each scan removes sample material. Under optimized conditions a dwell time of 10 ms per pixel was chosen resulting in an image scan time of about 44 min. A long-term experiment of about 11 h 40 min showed that 16 scans were possible without complete consumption of the sample. However, already accumulation of 5 image scans enabled a sensitive arsenic detection in a reasonable analysis time of about 3 h 40 min while only a part of the sample was consumed.

Sub-cellular elemental imaging

Figures 3i-iii show high resolution imaging of a *L. digitata* cell by NanoSIMS. Both, carbon and nitrogen (via CN^- detection) mapping display the thick cell walls/intercellular material. The high amount of polysaccharides in these structures explains the intense carbon signal, although the cells are also embedded in a carbon containing resin matrix. The detection of nitrogen in the cell wall could indicate the presence of proteins. Nitrogen mapping showed subcellular structures, especially chloroplasts were clearly visible, probably due to higher protein concentration in the chloroplasts compared to the cytosol.

In Figure 3ii sulphur was mainly found in the thick cell walls. This intense sulphur signal can be related to the presence of fucoidans, the sulphated polysaccharides typically found in

seaweed cell walls of brown algae such as *L. digitata*[xix]. Moreover, sulphur was also detected in the chloroplast which can be explained by sulphur-containing proteins involved in photosynthesis, such as ferredoxin and iron-sulphur clusters.

The phosphorous image is an accumulation of 5 scans. P was detected in concentrated small spots inside the cell which can be related to in 0.5-1 µm sized vacuoles, which can be seen as electronically dense sub-cellular structures in the TEM image (Figure 2). In green algae such small vacuoles are known to be acidocalcisomes containing polyphosphate and calcium and are involved in osmoregulation.[xx,xxi,xxii] Although those acidocalcisomes have never been identified in brown algae, they have been found in bacteria to human cells, which make them likely to occur in *L. digitata*. Moreover, phosphorus was clearly detected in the phospholipid containing cell membranes adjacent to the cell walls.

In Figure 3iii arsenic was found in a pattern consistent with the cell wall/intercellular material. The image is an accumulation of 5 scans. Figure 3iii (b and c) are a colour merge images of the relative distribution of arsenic (white) and nitrogen (red) or phosphorus (blue). It further demonstrates that the arsenic is mainly present in the cell wall with phosphorus outlining the cell membranes and subcellular structures.

Knowing the arsenic speciation in *L. digitata*, it is not expected that all arsenic would be in the cell membrane, since only a small proportion of arsenic is lipophilic (1.5%). Almost all arsenic is in the form of either inorganic arsenic or in the form of hydrophilic arsenosugars (together approx. 82%). No arsenic was detected inside the cells by NanoSIMS in either the cytosol, the vacuoles or acidocalcisomes (their location was indicated by the phosphorus map). Hence, the localisation of arsenic in *L. digitata* is significantly different to the accumulation of arsenic in rice root cells.[xxiii] Inorganic arsenic in rice roots is bound mainly to phytochelatins while DMA seemed unbound.[xxiv] In contrast brown seaweed with a large proportion of inorganic arsenic (*Hijiki* spp.) showed no significant amounts of arsenic phytochelatin complexes.[xxv] Hence, the lack of arsenic in the cytosol and in particular in the vacuoles of *L. digitata* is not surprising.

It seems that most arsenic is located in the cell walls containing polysaccharides such as alginate, fucoidan and cellulose. Those alginates are also known to accumulate mono and divalent cations such as Na^+, K^+, Ca^{2+}, but also Zn^{2+} and Cu^{2+}.[xiv] Arsenic however in its inorganic forms is either neutral ($As(OH)_3$) or anionic ($HAsO_4^{2-}$) and will not bind to the alginates in the same way. So far it is not known if arsenate or arsenite bind to either alginates

or fucoidans, which are abundant in the cell walls in brown seaweed. The fucoidans however bind sulphate as sulfuric acid ester. If arsenic binds as arsenate to the carbohydrate in a similar way is unclear. The resulting arsenic acid esters would be very unstable and will quickly hydrolyse and form again inorganic arsenic.[xxvi] It has been noted that not only AsHC and AsPL can be extracted, some unstable arsenic species have also been extracted with DCM/MeOH. A significant part of the extract eluted however in the void of a reverse phase HPLC method. This was likely to be attributed to unstable non-polar arsenolipids as shown before.[xxvii] Arsenic acid esters would quickly hydrolyse to inorganic arsenic during the sample preparation step.

Although the binding of arsenite or arsenate to the constituents of the cell wall and membrane is unclear, the accumulation of arsenate into the cell wall is however mechanistically conceivable. The arsenic accumulation into brown seaweed depends on the salinity and hence also on the arsenic concentration in the seawater.[xxviii] Arsenate might directly accumulate from seawater or indirectly when it is taken up through phosphate transporters and then excreted as arsenite. Efflux of arsenite is well known, while the efflux of arsenate has only recently been suggested to occur as well.[xxix]

The accumulation of arsenosugars in the cell wall is however more difficult to understand. Since no arsenosugars have been found in seawater so far, the accumulation of these arsenic species need to come from biotransformation reactions either directly within the macroalgae or from bacteria on the surface of the seaweeds.[xxx] If the arsenosugars are transported through the cell membrane into the cell wall, then certain transporters which excrete those compounds need to exist. Otherwise, the arsenosugars could be linked to the alginates which are produced in the Golgi apparatus and then directly incorporated into the carbohydrate structure. They might bind directly to the carbohydrates via the alcohol groups or the sulfonate (major arsenosugar in *L. digitata* is the AsSugar-SO_3). These compounds again would be rather unstable in water and hydrolyse quickly. The fact that no hotspot inside the cell which could be assigned to the Golgi apparatus has been found, indicates that the arsenic transformation inside the cell needs to be fast. Alginate generation is taking place within 20 minutes. This would explain that the cytosol and the sub-cellular structures inside the cell are virtually arsenic free.

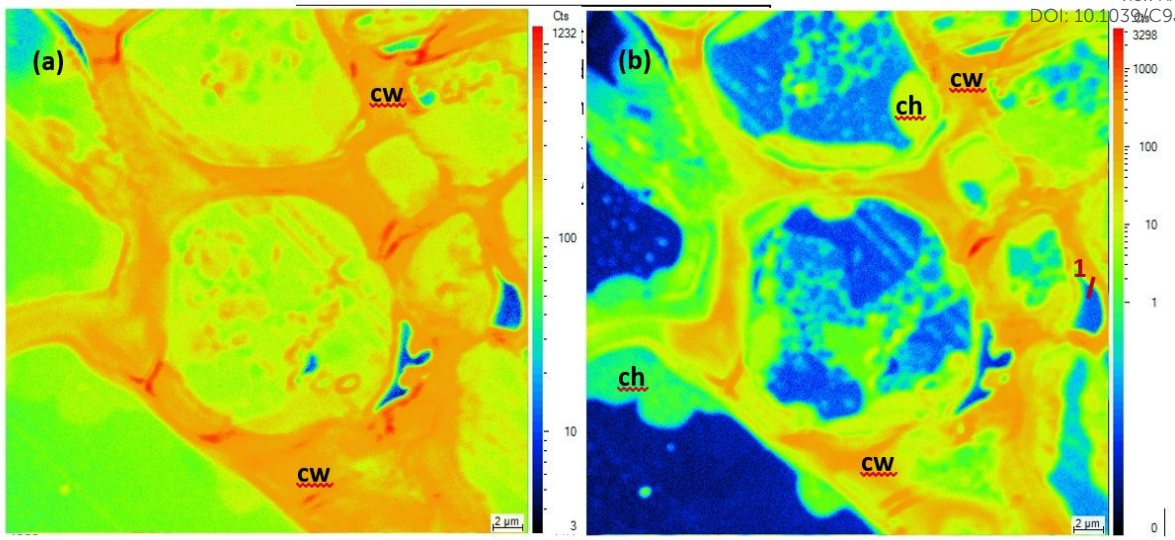

Figure 3i. High resolution imaging of carbon (via C_2^-) (a) and nitrogen (via CN^-) (b) in L. digitata cells by NanoSIMS obtained from a 300 nm resin section. Both images display the thick cell walls (cw). N mapping (b) shows subcellular structures, e.g. chloroplasts (ch), line scan 1 (red line) resulted in a measured lateral resolution of 305 nm. NanoSIMS images were obtained with an Cs^+ plasma primary ion source for detection of negative secondary ions: 35 x 35 µm^2 field of view images; 512 x 512 pixel; dwell time 10 ms/pixel; total image acquisition time approx. 44 min.

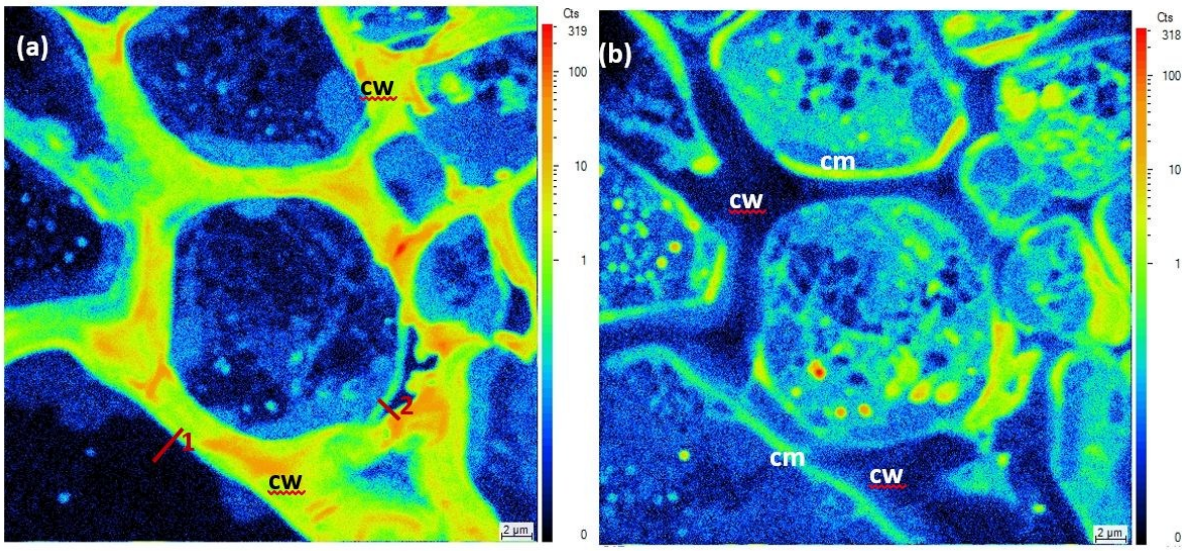

Figure 3ii. High resolution imaging of S (a) and P (b) in L. digitata cells by NanoSIMS obtained from a 300 nm resin section. S is mainly concentrated in the thick cell walls/intercellular material (cw). P is more concentrated in spots inside the cells as well as in the cell membrane (cm) adjacent to the cell wall. Line scans 1 and 2 (red lines) resulted in measured lateral resolutions of 433 nm and 295 nm, respectively. NanoSIMS images were

View Article Online
DOI: 10.1039/C9JA00187E

obtained with an Cs^+ plasma primary ion source for detection of negative secondary ions: 35 x 35 μm^2 field of view images; 512 x 512 pixel; dwell time 10 ms/pixel; total image acquisition time approx. 44 min.

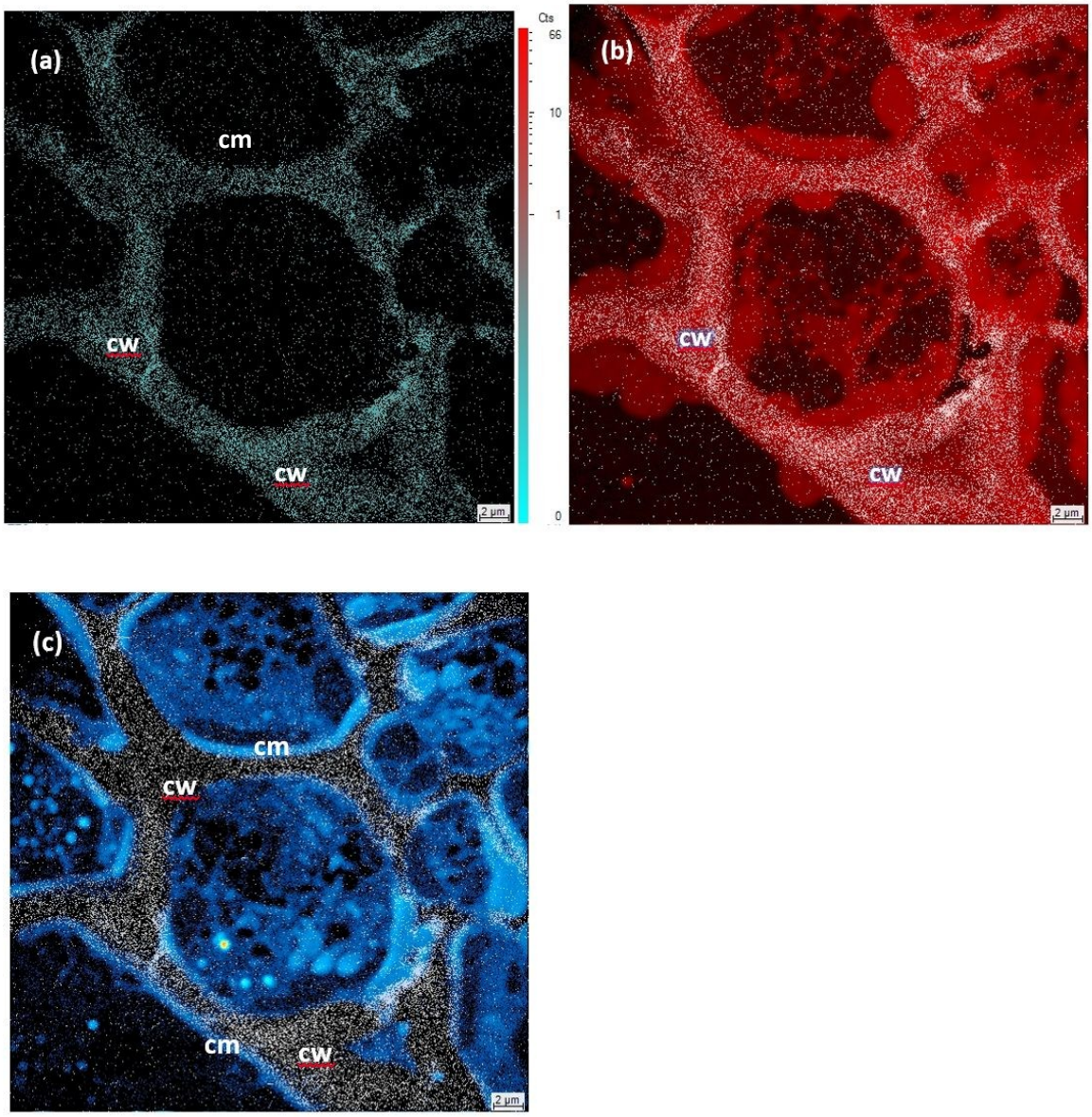

Figure 3iii. High resolution accumulated imaging of As (a) in L. digitata cells and two colour merge images that shows the relative distribution of As (white) and N (red) localisation (b) as well as As (white) and P (blue) localisation (c) by NanoSIMS obtained from a 300 nm resin section. As was mainly found in the cell wall/intercellular material (cw) and to a much lesser extend in the cell membrane (cm). NanoSIMS images were obtained with an Cs^+ plasma primary ion source for detection of negative secondary ions: 35 x 35 μm^2 field of view images; 512 x 512 pixel; dwell time 10 ms/pixel; total image acquisition time approx. 44 min.

It has been speculated that arsenosugars are intermediates in the formation of arsenolipids such as AsPL.[ii] But when arsenosugars accumulate in large quantities in the cell wall, then the biosynthesis to AsPL needs to take place there as well, which is unlikely. Hence, the localisation of arsenic in the cell wall rather than in the cell membrane indicates that the seaweed can handle certain concentrations of arsenic and has means of excluding the arsenic from the cytosol and other sub-cellular structures within the cell. The biotransformation and kinetics of arsenic in *L. digitata* are not clear, but the seaweed is able to biotransform quickly the taken up arsenic and transport it outside the cell. This could be an effective detoxification strategy, or the evidence of the utilization of the accumulated arsenic for a purpose, since the cell wall with the gel-like alginates and sulphated fucoidans act often as the first barrier to toxic or unwanted chemicals. More fundamental studies are necessary to elucidate the biochemical role of arsenic in seaweed.

In summary the complimentary use of high spatial resolution imaging of elements at a sub-cellular level in combination of speciation analysis can shed new lights on the role of arsenic in seaweeds. Is the arsenic in the form of inorganic arsenic essential for the algae as suggested elsewhere[xxxi] or is the efflux of arsenic in these molecular forms into the intercellular space or the cell wall a successful detoxification strategy? These questions can only be asked if in addition to arsenic speciation also its distribution within a cell and sub-cellular structures is known this however would need a high resolution imaging technique which is capable at the same time to provide speciation information. μ-XANES would have the analytical attributes but its resolution is currently not sufficient to identify subcellular structures.

References

[i] H.R. Hansen, A. Raab and J. Feldmann, *J. Anal. At. Spectrom*. 2003, **18**, 474-479.

[ii] X.M. Xue, J. Ye, G. Raber, B.P. Rosen, K. Francesconi, C. Xiong, Z. Zhu, C. Rensing, and Y.G. Zhu, *Environ. Sci. Technol.* 2019, **53**, 634-641.

[iii] W. Maher and E. Butler, *Appl. Organmet. Chem.,* 1988, **2**, 191-214.

[iv] J. Feldmann and E.M. Krupp, *Anal. Bioanal. Chem.*, 2011, **399**, 1735-1741.

[v] S. Garcia-Salgado, G. Raber, R. Raml, C. Magnes and K.A. Francesconi, *Environ. Chem.*, 2012, **9**, 63-66.

View Article Online
DOI: 10.1039/C9JA00187E

[vi] A. Raab, C. Newcombe, D. Pitton, R. Ebel, and J. Feldmann, *Anal. Chem.* 2013, **85**, 2817-2824.

[vii] K. Hanaoka, K. Yosida, M. Tamano, T. Kuroiwa, T. Kaise and S. Maeda, *Appl. Organomet. Chem.*, 2001, **15**, 561-565.

[viii] J.M. Ronan, D.B. Stengel, A. Raab, J. Feldmann, L. O'Hea, E. Bralatei and E. McGovern. *Chemosphere* 2017, **186**, 17-23.

[ix] E. Bralatei, K. Nekrosuite, J. Ronan, A. Raab, E. McGovern, E.M. Krupp and J. Feldmann, *Microchim. Acta* 2017, **184**, 1701-1709.

[x] A.H. Petursdottir, N. Friedrich, S. Musil, A. Raab, H. Gunnlaugsdottir, E.M. Krupp and J. Feldmann, *Anal. Met.* 2014, **6,** 5392-5396.

[xi] K.O. Amayo, K.O, A.H. Petursdottir, C. Newcombe, H. Gunnlaugsdottir, A. Raab, E. Krupp, and J. Feldmann, *Anal. Chem.* 2011, **83**, 3589-3595.

[xii] A. Raab, C. Newcombe, D. Pitton, R. Ebel and J. Feldmann, *Anal. Chem.* 2013, **85**, 2817-2824.

[xiii] S. Schiewer and B. Volesky, Biosorption by marine algae. In: Valdes JJ, editor. Remediation. Dordrecht, The Netherlands: Kluwer Academic Publishers; 2000.p. 139–69.

[xiv] T. A. Davis et al., A review of the biochemistry of heavy metal biosorption by brown algae. *Water Res.* 2003, **37**, 4311–4330.

[xv] W. Mackie and R.D. Preston. Cell wall and intercellular region polysaccharides. In: W.D.P. Stewart, editor. Algal physiology and biochemistry. Oxford, UK: Blackwell Scientific Publications; 1974. p. 58–64.

[xvi] K. L. Moore, M. Schroder, Z. Wu, B. G. H. Martin, C. R. Hawes, S. P. McGrath, M. J. Hawkesford, J. Feng Ma, F.-J. Zhao, and C. R. M. Grovenor, *Plant Physiol.*, 2011, **156**, 913–924.

[xvii] H. Jiang, C. N. Goulbourne, A. Tatar, K. Turlo, D. Wu, A. P. Beigneux, C. R. M. Grovenor, L. G. Fong, and S. G. Young, *J. Lipid Res.*, 2014, **55**, 2156–2166.

[xviii] Malherbe, J., Penen, F., Isaure, M.-P., Frank, J., Hause, G., Dobritzsch, D., Gontier, E., Horreard, F., Hillion, F., Schaumloeffel, D., *Anal. Chem.* 2016, **88,** 7130–7136

[xix] A. Synytsya, J. Čopíková, W.J. Kim, Y.I. Park. (2015) Cell Wall Polysaccharides of Marine Algae. In: Kim SK. (eds) Springer Handbook of Marine Biotechnology. Springer Handbooks. Springer, Berlin, Heidelberg.

[xx] N. Lander, C. Cordeiro, G. Huang and R. Docamo, *Biochem. Sco. Trans.* 2016, **44**, 1-6.

[xxi] F. Penen, M.P. Isaure, D. Dobritzsch, I. Bertalan, H. Castillo, O. Proux, E. Gontier, P. Le

View Article Online
DOI: 10.1039/C9JA00187E

Coustumer and D. Schaumlöffel, *Metallomics* 2017, **9**, 910-923.

[xxii] F.A. Ruiz, N. Marchesini, M. Seufferheld, Govindjee and R. Docampo, *J. Biol. Chem.*, 2001, **276**, 49196-46203.

[xxiii] K.L. Moore, M. Schroder, E. Lombi, F.J. Zhao, S.P. McGrath, M.J. Hawkesford, P.R. Shewry and C.R.M. Grovenor, *New Phytol.* 2010, **185**, 434–445.

[xxiv] B.L. Batista, M. Nigar, A. Mestrot, B.A. Rocha, F. Barbosa Jr, A.H. Price, A. Raab and J. Feldmann, *J. Exp. Bot.,* 2014, **65**, 1467-1479.

[xxv] B.A. Wood, A.A. Meharg, S. Miyashita, T. Kaise, A. Raab and J. Feldmann, *Environ. Chem.* 2011, **8**, 30-43.

[xxvi] F.H. Westheiner, *Science* (1987) **235,** 1173-1178.

[xxvii] A.H. Petursdottir, J.R. de Jesus, H. Gunnlaugsdottir and J. Feldmann, *J. Anal. At. Spectrom*., 2018, **33**, 102-110.

[xxviii] E. Ownsworth, D. Selby, C.J. Ottley, E.Unsworth, A. Raab, J. Feldmann, A.D. Sproson, J. Kuroda, C. Faidutti and P. Bücker, *Sci. Tot. Environ.*, 2019, 685, 259-272.

[xxix] L.D. Garinski, B.P. Rosen and J. Chen, *Environ. Intern.*, 2019, **126**, 585-597.

[xxx] A.H. Petursdottir, J. Bladgen, K. Gunnarsson, A. Raab, D.B. Stengel, J. Feldmann, H. Gunnlaugsdottir, *Anal. Bioanal. Chem*., 2019, **411**, 4973-4985.

[xxxi] A.H. Petursdottir, K. Fletcher, H. Gunnlaugsdottir, E. Krupp, F. Kuepper, J. Feldmann, *Environ. Chem.,* 2015, **13**, 21-33.

View Article Online
DOI: 10.1039/C9JA00187E

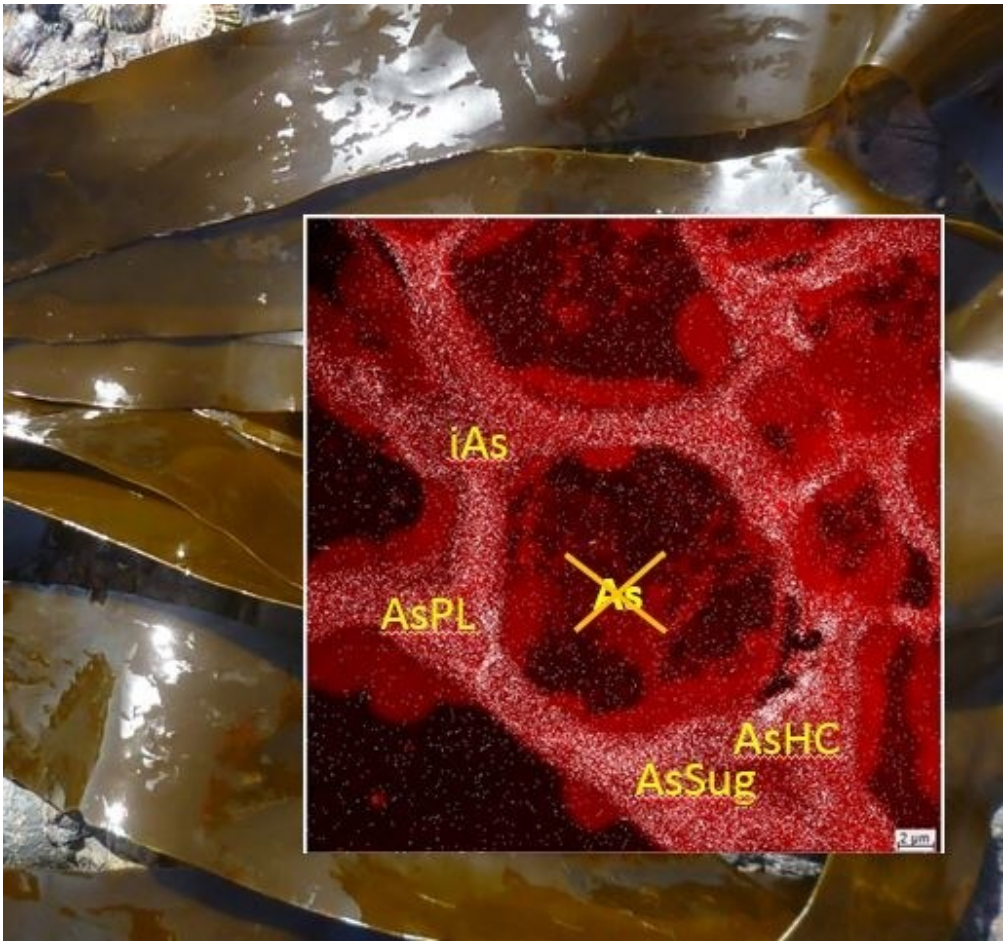

108x101mm (120 x 120 DPI)